Observation of resistivity minimum at low temperature in Co_xCu_{1-x} ($x \sim 0.17$–0.76) nanostructured granular alloys

S. Dhara, R. Roy Chowdhury, and B. Bandyopadhyay*
Saha Institute of Nuclear Physics, 1/AF Bidhannagar, Kolkata-700064, India
(Received 24 February 2016; revised manuscript received 23 May 2016; published 14 June 2016)

Electrical resistivity of nanostructured granular alloys Co_xCu_{1-x} ($x \sim 0.01$–0.76) prepared by the chemical reduction method is investigated in the temperature range 2–300 K. The samples with a low cobalt content of $x \leqslant 0.1$ show a metallic resistivity behavior. For samples with a higher cobalt content, $x \geqslant 0.17$, the resistivity shows a minimum. The minimum becomes more pronounced as Co content (x) increases and also as the temperature of minimum resistivity, T_{min}, increases with x. The resistivity minimum is obtained in this magnetic alloy system even for a cobalt concentration as high as ∼76%. Application of an external magnetic field has a negligible effect on the resistivity behavior. Detailed analysis suggests that the low-temperature upturn in resistivity most probably arises due to elastic electron-electron interaction (the quantum-interference effect). Magnetic measurements at 4 K on the same samples show the absence of long-range magnetic interaction and evidence of increasing magnetic disorder as x increases beyond ∼10%. Combining the results of the two types of measurements, a model of formation of these alloy particles involving random clusters of Co atoms within the Cu matrix has been proposed.

DOI: 10.1103/PhysRevB.93.214413

I. INTRODUCTION

Granular alloys are mostly obtained in systems of immiscible elements, e.g., a magnetic d-element and a noble metal. Such materials are readily recognized for their giant magnetoresistance (GMR), as found in alloys of Co-Cu, Co-Ag, Fe-Cu, Fe-Ag, etc. [1–7], where spin-dependent scattering of electrons plays a very significant role. Even before GMR, such alloys exhibited anomalous resistivity behavior at low temperature, which was explained in terms of Kondo-like scattering of electrons by clusters of localized magnetic moments [8–10]. The Kondo theory [11] initially developed to explain the resistivity minimum in dilute magnetic alloys was later extended to dense localized moment systems, in particular to explain the transport properties in intermetallic compounds of Ce and Yb [12–17]. But generally in a dense system beyond a certain concentration of local moments, the long-range magnetic interaction overcomes the Kondo effect [18]. Nevertheless, the resistivity minima obtained for rather high local moment concentrations, e.g., up to ∼45% of Ni in Ni-Au [9] and 10–15 % of Co in Co-Cu [19], were explained in terms of Kondo scattering. On the other hand, apart from alloys and intermetallics, the ceramic samples and other compounds exhibit low-temperature resistivity upturns, which are explained by alternative mechanisms, such as electron-electron interaction, the weak localization effect (due to the finite-size effect), spin-polarized tunneling through grain boundaries [20–27], etc. Experimentally, the prevalence of one or another of these mechanisms is manifested through the magnetic-field dependence of the resistivity behavior around the temperature (T_{min}) of minimum resistivity.

We have performed detailed resistivity measurements on Co-Cu alloys in a wide range of compositions, and we concluded that the low-temperature resistivity upturn obtained in samples with $x \geqslant 0.17$ is arising due to electron-electron Coulomb interaction (CI). To establish the feasibility of such a conclusion, we have presented here briefly the magnetization results on the same samples.

II. EXPERIMENT

Inhomogeneous nanostructured cobalt-copper alloys of varying compositions that can be denoted as Co_xCu_{1-x} ($x \sim 0.01$–0.7) were prepared by chemical reduction of $CoCl_2$ and $CuCl_2$ in a solution that also contained 0.05 mM of cetyltrimethyl ammonium bromide (CTAB), which was used for capping of the alloy particles. The details of sample preparation and characterization have been reported previously [28]. The average cobalt content (x) in these alloys was obtained from inductively coupled plasma optical emission spectroscopic (ICPOES) measurements, and it is given in Table I. Transmission electron microscopy (TEM) results [Fig. 1(a)] show particles of mean size ∼15 nm existing in lumps and filament-like formations. For further studies, the samples were pressed into pellets measuring 13 mm in diameter and ∼1 mm in thickness using a KBr pellet die under pressure of 0.33 GPa in a laboratory press. The pellets were annealed for 1 h at 200 °C in a reducing atmosphere. For resistivity measurements, the pellets were cut into rectangular pieces that were measured and weighed for density estimation. The density of the pellets ranged between 30% and 50% of the theoretical value, with a minimum value of 2.7 ± 0.05 g/cm^3 obtained for the Co-0.45 sample. These values are typical of pellet samples obtained only by cold compaction, without additional compaction by means of thermal treatment [29].

Powder x-ray diffraction (XRD) studies of the pallets were performed to ascertain the quality of the samples. Though the entire sample preparation procedure was carried out under inert gas and reducing atmosphere, some amount of oxidation during transfer of samples could not be avoided. The analysis of XRD data [Fig. 1(b)] showed that some of the low cobalt-containing samples had Cu_2O not exceeding 5%

*bilwadal.bandyopadhyay@saha.ac.in

TABLE I. The actual values obtained from ICPOES studies of average cobalt content in mol % in Co_xCu_{1-x} samples, which are denoted as Co-x.

Sample Co-x	Co mol %
Co-0.01	1.20(1)
Co-0.03	3.41(1)
Co-0.05	5.67(1)
Co-0.08	8.02(1)
Co-0.10	10.48(1)
Co-0.17	17.87(1)
Co-0.32	31.96(1)
Co-0.45	44.93(1)
Co-0.56	56.01(1)
Co-0.76	76.73(1)

of the sample volume. Higher cobalt-containing samples were comparatively free of oxidation.

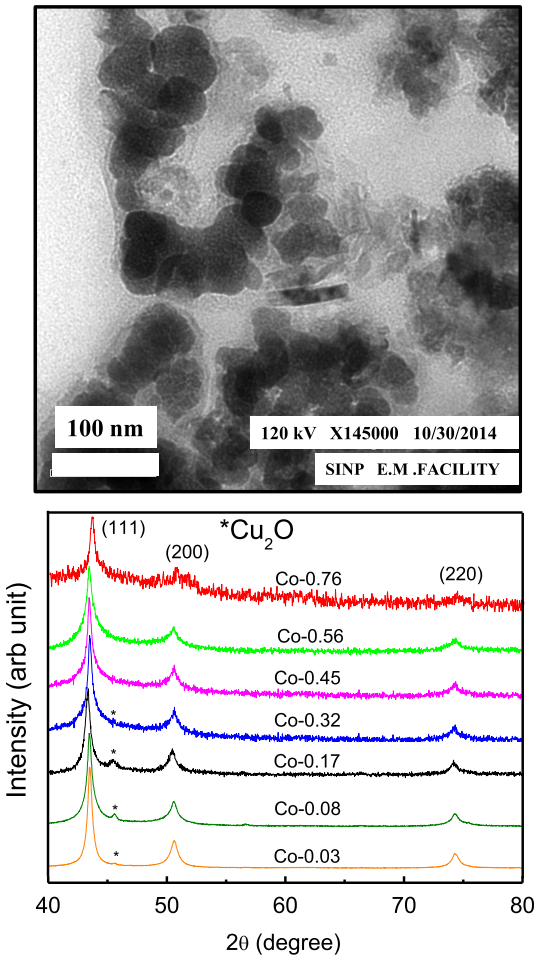

FIG. 1. (a) Transmission electron micrograph (TEM) of the sample Co-0.5, and (b) room temperature powder x-ray diffraction (XRD) pattern of Co-x samples. The Miller indices correspond to the fcc lattice as in copper.

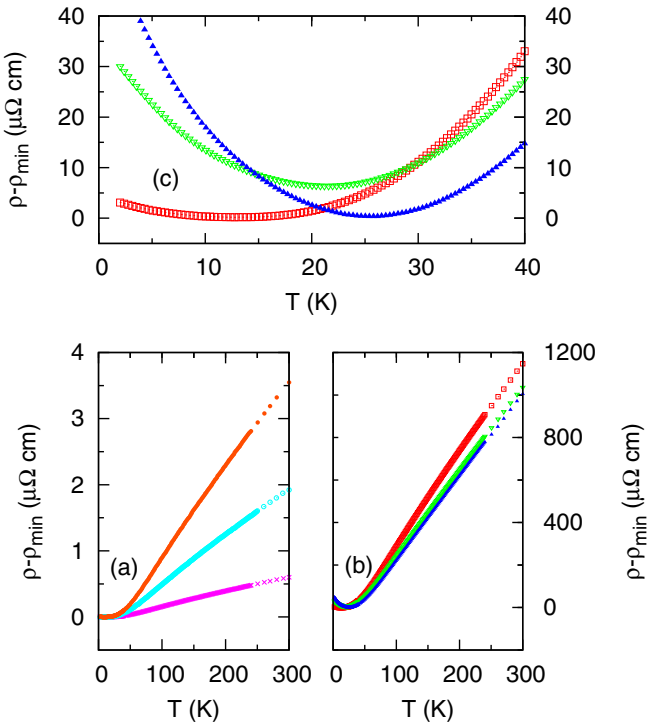

FIG. 2. Resistivity (ρ) as a function of temperature for (a) samples Co-0.01 (×), Co-0.03 (○), and Co-0.08 (●); (b) samples Co-0.17 (□), Co-0.56 (▽), and Co-0.76 (▲); and (c) expanded low-temperature region of Fig. 2(b).

III. RESULTS AND DISCUSSION

A. Resistivity measurements

Resistivity measurements were performed with a Physical Properties Measurement System (PPMS 9 of Quantum Design) using a four-probe method and a constant current of 60 mA. Figures 2(a) and 2(b) show resistivity as a function of temperature (ρ) in between 2 and 300 K in zero external magnetic field for some of the samples. For convenience, ($\rho - \rho_{\min}$) is plotted in this figure. For low Co-containing samples, Co-0.01, Co-0.03, and Co-0.08, a metallic resistivity behavior is observed. It decreases as temperature decreases from 300 K down to ∼10 K, and there is a residual resistivity below 10 K where ($\rho - \rho_{\min}$) levels off to zero [Fig. 2(a)]. For higher Co-containing samples, Co-0.17, Co-0.56, and Co-0.76 [Fig. 2(b)], the resistivity is much higher and the zero in ($\rho - \rho_{\min}$) is obtained at a finite temperature $T_{\min}$, which is seen clearly in Fig. 2(c). Figure 2(c) shows that $T_{\min}$ increases with x, and also the minimum becomes more pronounced with x, i.e., the depth of the resistivity minimum, which may be defined as ($\rho_{5\,\mathrm{K}} - \rho_{T_{\min}}$), increases with x.

The resistivity for a metallic behavior can be written in the form of a general power law, $\rho = \rho_0 + \rho_P T^P$, in which ρ_0 is the residual resistivity and the other term represents the combined effect of inelastic electron-electron, electron-phonon, and electron-magnon scattering contributions. In granular alloys and other systems, the resistivity upturn in low temperature can have its origin in different mechanisms such as the Coulomb blockade effect [30], electron-electron scattering, and the Kondo effect. For the Coulomb blockade

(CB) effect, the resistivity is empirically given as

$$\rho = \rho_0 + \rho_{\rm CB} \exp\left(\frac{\Delta}{T}\right)^{1/2} + \rho_P T^P, \quad (1)$$

where Δ is the Coulomb energy required to generate a charge carrier, in which an electron is removed from a neutral grain and placed on a neighboring neutral grain [31].

An upturn in resistivity may also result from tunneling of spin-polarized conduction electrons between neighboring grains whose magnetic moments are not parallel [32],

$$\rho = \frac{r_1 + r_2 T^{3/2}}{1 + \epsilon \langle \cos\theta_{ij} \rangle}. \quad (2)$$

In the above equation, r_1 and r_2 are field-independent parameters and ϵ represents the degree of polarization of electrons. In the absence of magnetic field, the spin-correlation function $\langle \cos\theta_{ij} \rangle$ is given as

$$\langle \cos\theta_{ij} \rangle = -L\left(\frac{|J|}{k_B T}\right),$$

where $L(x) = [\coth(x) - 1/x]$ is the Langevin function and J' is the intergrain antiferromagnetic exchange integral.

With the assumption that the upturn is due to the Kondo effect, the resistivity at low temperatures can be written as [10]

$$\rho = \rho_0 - \rho_K(T) + \rho_P T^P, \quad (3)$$

where $\rho_K(T) = c\rho_m + c\rho_1 \ln T$. ρ_m is the spin-scattering resistivity and $\rho_1 = \rho_m \frac{(3n_s J_{sd})}{E_F}$, where J_{sd} is the s-d exchange interaction between the spins (S_e) of the conduction electrons of Cu and the localized magnetic moment (S_d) of the transition element Co. E_F is the Fermi energy of cobalt, and n_s is the number of conduction electrons per atom.

Various nonmagnetic and magnetic amorphous and disordered metal alloys exhibit the resistivity minimum at low temperature [33–35]. The origin of the minimum in these strongly disordered systems has been attributed to the elastic electron-electron interaction and the quantum coherence effect [36], in which the resistivity in the low-temperature regime

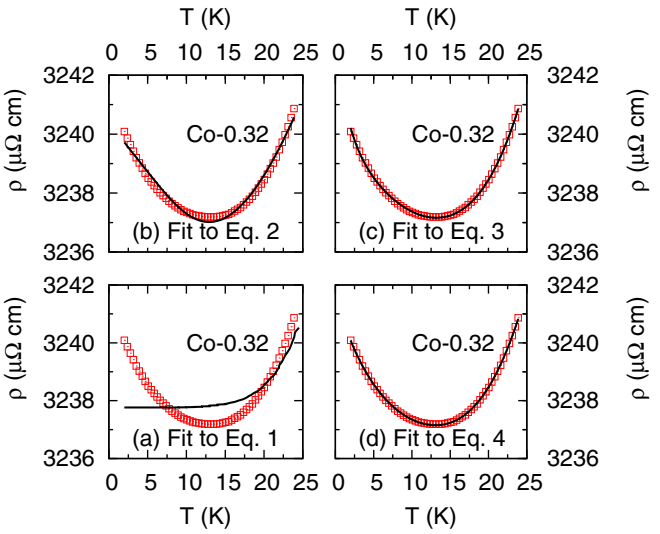

FIG. 3. Fitting of low-temperature resistivity upturn of the Co-0.32 sample. The experimental data (□) are fitted (solid line) for (a) the Coulomb blocking effect [Eq. (1)]; (b) intergrain tunneling of electrons [Eq. (2)]; (c) the Kondo effect [Eq. (3)]; and (d) elastic scattering of electrons [Eq. (4)].

takes the form

$$\rho = \rho_0 - \rho_e T^{1/2} + \rho_P T^P. \quad (4)$$

In the above equation, ρ_e, the elastic scattering coefficient is given as [22]

$$\rho_e = 0.0309 \frac{\rho_0^2 e^2}{\hbar}\left(\sqrt{\frac{1}{T L_T^2}}\right), \quad (5)$$

where L_T is the thermal diffusion length, which, for any temperature (T), can be obtained from ρ_e and ρ_0 estimated from fitting of the experimental data with Eq. (4).

Equations (1)–(4) have been used to fit the observed resistivity data. An example is shown in Fig. 3 for the fitting of the data of the Co-0.32 sample. It is found that at low temperatures the data do not fit at all to Eq. (1), and they make an unsatisfactory fit to Eq. (2). However, the data fit equally satisfactorily to Eqs. (3) and (4). The data for all the samples $x \geqslant 0.17$ were fit with Eqs. (2)–(4), and also the magnetic-field dependence of resistivity was checked to ascertain the plausible mechanism behind the observed resistivity minimum. Table II gives the experimentally obtained temperature of minimum resistivity,

TABLE II. For Co_xCu_{1-x} ($0.17 \leqslant x \leqslant 0.76$), the temperature of minimum resistivity ($T_{\rm min}$) and various parameters obtained from fitting the experimental data with equations corresponding to intergrain tunneling [Eq. (2)], Kondo scattering [Eq. (3)], and elastic scattering [Eq. (4)] of electrons. Also given are the thermal diffusion lengths (L_T) at 10 K calculated as mentioned in the text.

		From Eq. (2)				From Eq. (3)			From Eq. (4)			
Sample	$T_{\rm min}$ (K)	r_1 ($\mu\Omega$ cm)	r_2 ($\mu\Omega$ cm)	ϵ	J/k_B (K)	ρ_0 ($\mu\Omega$ cm)	ρ_1 ($\mu\Omega$ cm)	ρ_P ($\mu\Omega$ cm)	ρ_0 ($\mu\Omega$ cm)	ρ_e ($\mu\Omega$ cm)	ρ_P ($\mu\Omega$ cm)	L_T (nm)
Co-0.17	13.5(5)	1359	0.5	0.01	0.03	1382	1.1	$<10^{-4}$	1383	1.3	2×10^{-4}	34
Co-0.32	13.5(5)	3196	1.1	0.01	0.03	3241	1.8	$<10^{-4}$	3244	2.6	2×10^{-4}	95
Co-0.45	16.5(5)	5268	2.8	0.02	0.03	5414	4.2	$<10^{-4}$	5418	8.9	2×10^{-4}	115
Co-0.56	21.5(5)	7425	2.8	0.02	0.03	7641	12.4	$<10^{-4}$	7606	11.1	0.003	125
Co-0.76	25.5(5)	10390	3.5	0.02	0.03	10663	23.5	3×10^{-4}	10669	19.3	0.018	140

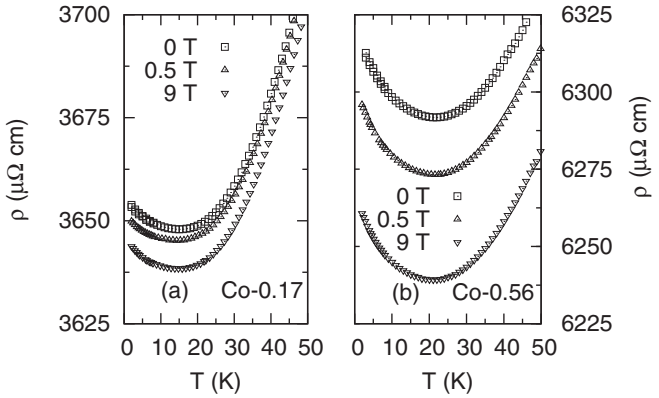

FIG. 4. (a) Resistivity (ρ) vs temperature in zero magnetic field and in magnetic fields of 0.5 and 9 T measured in samples (a) Co-0.17 and (b) Co-0.56.

T_{min}, and the various fitting parameters corresponding to each equation. The results show that the values of electron polarization (ϵ) and intergrain coupling (J) obtained from the fitting with Eq. (2) are too small to consider the electron tunneling effect to be responsible for the resistivity behavior. Also, in cases in which the intergrain tunneling effect is dominant, the depth of the minimum in resistivity decreases upon increasing the magnetic field, and the minimum vanishes beyond a certain value of the magnetic field [37,38]. In Fig. 4, the zero-field resistivities of two of these samples, viz., Co-0.17 and Co-0.56, are shown with the resistivities measured in magnetic fields of 0.5 and 9 T. It is found that the resistivity minimum is not suppressed even at high magnetic fields. Previously, such low-temperature upturns in granular alloys of Au-Ni and Co-Cu were explained by the Kondo scattering mechanism involving small clusters of spins, and it was also observed [19] that for larger cluster sizes the Kondo effect should disappear. Contrary to this observation, the resistivity upturn in the present case is very much pronounced at high Co concentrations, and at low Co concentrations it is not obtained. Moreover, the Kondo effect is weakened in the presence of a magnetic field. It is indicated from the data of Fig. 4 that magnetic fields have a negligible effect on both T_{min} and the depth of the resistivity minimum. In other words, these samples possess small magnetoresistance, $\sim -0.4\%$ near T_{min} at 9 T. These observations strongly suggest that the influence of both intergrain tunneling [32] and Kondo-like scattering of electrons is absent in the present case, and the observed resistivity minimum may arise from elastic scattering of electrons. Also, it is seen in Table II that ρ_P is orders of magnitude smaller than other resistivity coefficients, indicating that inelastic scattering of electrons does not have a significant contribution to resistivity at these temperatures. The values of P, not shown in Table II, are varying in the range 3.2–4.2.

The resistivity upturn resulting from Coulomb interaction is due to the quantum-interference effect of the electrons. Electrons travel with a characteristic mean free time, τ_e, and mean free path, l_e, between two successive collisions. For elastic scattering, the electrons remain coherent even for distances larger than l_e as energy is conserved. The temperature effect can cause destruction of this quantum coherence of electrons. At low temperatures, the thermal energy is much smaller than the Fermi energy, and the wave functions of the electrons maintain their amplitudes, although the phases vary slightly. If this variation is sufficiently small, thermal energy is unable to destroy the coherence. Under this condition, the electrons move coherently a long distance. With an increase in Co concentration, the number of scatters in the path of the coherently mobile electron increases, and thus coherent scattering events increase as well. This results in an increase of T_{min}, ρ_e, and also of L_T with an increases in Co concentration. At temperatures above T_{min}, the coherence is lost and the resistivity increases with increasing temperature.

Table II lists the residual resistivities (ρ_0) for the samples with $x \geqslant 0.17$ only; however, ρ_0 for low Co-containing samples has also been obtained. A pellet of copper-only nanoparticles prepared by an identical procedure (i.e., the $x = 0$ sample in the present series) shows metallic behavior and yields a ρ_0 of 56 $\mu\Omega$ cm, which is high compared to ρ_0 of 7 $\mu\Omega$ cm obtained in a melt-spun CoCu alloy [39]. This increment is probably related to the lump and filament structure [Fig. 1(a)] that results in electron flow in narrow meandering channels having a typical width of the order of the particle size, and the resistivity predominantly arises from diffusive scattering at the channel boundaries [40]. In the case of alloys, we have found that in low Co samples, ρ_0 remains small and close to that of the Cu only sample. But as x increases beyond 0.1, ρ_0 increases continuously and almost linearly with x throughout the range $0.17 \leqslant x \leqslant 0.76$. This systematic variation of ρ_0 most probably reflects a variation in the electron diffusion or scattering mechanism that depends only on cobalt concentration. However, the huge values of ρ_0, more than two or three orders of magnitude over the values for pure Cu or low cobalt-containing bulk alloy, is probably related to the microstructure of the system [29].

It is surprising that the resistivity minimum originating from electron-electron interaction is sustained to a very high concentration of Co (Co $\sim$76%). Generally in a dense alloy system, the magnetic impurities cannot remain isolated and there appears a long-range magnetic interaction that dominates *e-e* interaction. This does not seem to happen in the present case. Indeed, our previous study [28] of magnetic measurements on a similar system of Co_xCu_{1-x} with $x \leqslant 0.3$ showed the absence of any long-range magnetic interaction and indicated that isolated nanoparticles are formed in a core-shell-type structure with cluster(s) of cobalt atoms surrounded by copper. The magnetization of the present samples has been studied in a similar manner as in Ref. [28], and the results are briefly described in the next section.

B. Magnetization measurements

Magnetic measurements were performed using a superconducting quantum interference device vibrating sample magnetometer (MPMS 7 of Quantum Design). The magnetization, M, as a function of temperature in between 4 and 380 K was measured in zero-field-cooled and field-cooled (ZFC-FC) conditions in a magnetic field, H, of 10 mT. In all samples, ZFC magnetization remains below FC magnetization, indicating superparamagnetic behavior. At any temperature, M versus H for all samples could be fitted as a sum of superparamagnetic

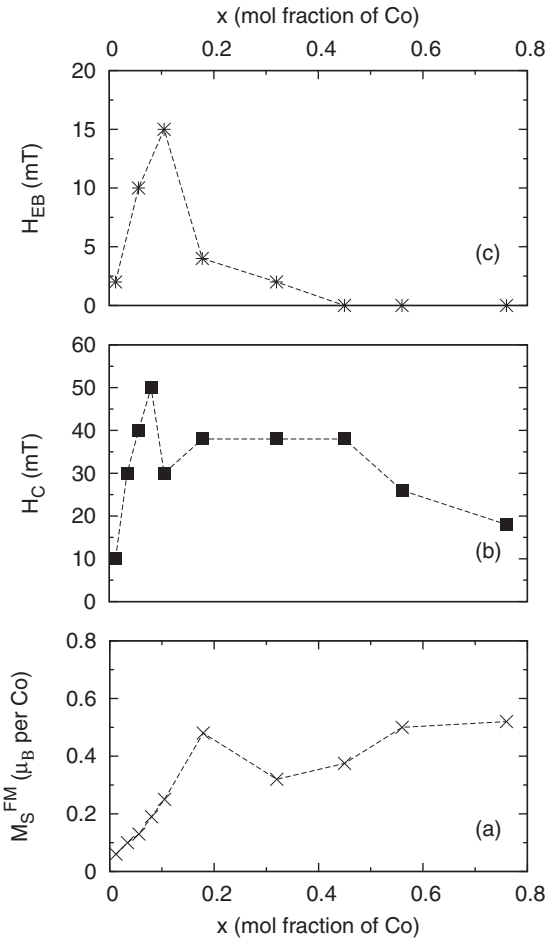

FIG. 5. (a) Ferromagnetic saturation moment (M_S^{FM}) vs x in Co_xCu_{1-x}, (b) coercivity (H_C) vs x, and (c) exchange bias (H_{EB}) vs x. The broken lines are a guide to the eye.

(SPM) and ferromagnetic (FM) components as given by

$$M(H) = M_S^{\mathrm{FM}} \tan^{-1} \chi H + M_S^{\mathrm{SPM}} \left[\coth\left(\frac{\mu H}{k_B T}\right) - \left(\frac{\mu H}{k_B T}\right)^{-1} \right]. \quad (6)$$

The first term is the FM component, with M_S^{FM} being the saturation magnetization, and it arises due to FM interaction within the Co atom cluster. The second term is the expression for the SPM component, with M_S^{SPM} being the corresponding saturation magnetization and μ the moment of a SPM cluster. In addition, all the samples exhibit a hysteresis loop and thus a coercive field (H_C) that decreases with temperature. The hysteresis loops were also obtained under field-cooled condition, i.e., after cooling the samples from room temperature in a 7 T magnetic field. For samples of $x \leqslant 0.32$, such hysteresis loops were asymmetric and shifted in the negative direction of the H axis, thus yielding an exchange bias field (H_{EB}). It has been argued that H_{EB} originates at the interface of the Co-rich core and the Cu-rich shell of the core-shell-type structure. Figure 5 shows the variations of M_S^{FM}, H_C, and H_{EB} with the Co content in all Co-x samples at 4 K.

In this figure, we see that in samples with $0.01 \leqslant x \leqslant 0.17$, M_S^{FM} increases with Co content. Further increasing the Co content, M_S^{FM} initially appears to decrease, but then it increases and tends to level off at values of $\sim 0.5\mu_B$/Co in Co-0.76. Even at this high cobalt-containing sample, the saturation magnetic moment of cobalt remains much smaller than the reported value, $2.2\mu_B$/Co, of Co nanoparticles. The result definitely shows that there exists no long-range magnetic interaction in this system of alloys. It may be mentioned here that a previous experiment [41] on one of these samples, namely $Co_{0.3}Cu_{0.7}$, yielded a strong magnetic memory effect at all temperatures 4–300 K as a consequence of the absence of long-range magnetic interaction. H_C initially increases rapidly with x and shows a peak value of $\sim$50 mT in Co-0.08, then it becomes smaller in $0.1 \leqslant x \leqslant 0.32$ with values $\sim$40 mT, and it tends to decrease as Co content increases further. H_{EB} also increases with x initially and has a maximum value of 15 mT in Co-0.10. It then decreases with increasing Co content and becomes negligibly small in $0.32 \leqslant x \leqslant 0.76$.

With the above magnetization results and the observation that the residual resistivity (ρ_0) is small for low Co-containing samples and then increases almost linearly with Co content, we can now construct a model for the formation of these noninteracting CoCu alloy particles (see in Fig. 6). At low Co concentrations (x), there are small cluster(s) of Co atoms surrounded by Cu on all sides. Electrical conduction in an assembly of such particles takes place mainly through copper, and there is no significant scattering by Co clusters. Thus, a small residual resistance is obtained. At intermediate Co concentrations, the cluster size increases with x, and as a consequence M_S^{FM}, H_C, and also H_{EB} increase. Afterward, when x goes above a value of $\sim$0.16, there is no further increase in the cluster size. Instead, there is an increase only in the number of clusters inside a particle by way of the formation of new clusters and also disintegration of existing clusters. In this condition, M_S^{FM} tends to level off, and, simultaneously, the boundary between Co clusters and the Cu shell may become diffused or less well-defined, resulting in the decrease and finally the disappearance of H_{EB}. Under such a condition, a high degree of structural and magnetic disorder is expected to prevail in the system. In an earlier resistivity study [42] on bulk Cu-Ni alloys, the increase of ρ_0 with Ni concentration was interpreted in terms of electron scattering by Ni clusters. Our results, therefore, indicate that for higher cobalt, the

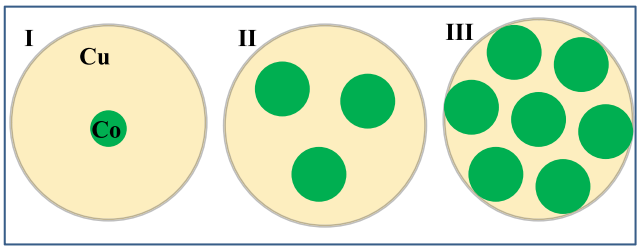

FIG. 6. A schematic diagram of a particle of the Co-Cu alloy with a low cobalt content (marked I), an intermediate cobalt content (marked II), and a high cobalt content (marked III) regions. The particle in all three cases is in the form of cluster(s) of Co atoms within the Cu matrix.

clusters may be at the periphery of the particles, and scattering from cobalt clusters dominates in the process of electron conduction (see Fig. 6).

IV. CONCLUSION

In summary, a detailed investigation of the temperature dependence of resistivity was carried out in the granular alloy system of Co_xCu_{1-x} with varying Co content $x \sim 0.01$–0.76. All the samples show metallic resistivity behavior below room temperature. A minimum in low-temperature resistivity was found only in high Co-containing samples. The resistivity behavior around the minimum is weakly dependent on magnetic field. It can be reasonably argued that the low-temperature resistivity upturn arises from the quantum-interference effect induced by inherent disorder of the system. Magnetization studies show that with increase in Co content, the magnetic disorder in the system increases and there is no interparticle long-range interaction even at high Co concentrations. The same sample conditions appear to facilitate the electron-electron elastic interaction, although the idea needs further explanation. It would be interesting to find out if a similar resistivity behavior is shown in identically synthesized binary alloys of other combinations, such as Fe-Cu, Ni-Au, Co-Ag, etc.

ACKNOWLEDGMENTS

The authors would like to thank Susanta Lahiri for the ICPOES measurements and Pulak Ray for TEM studies. The authors also thank Indranil Das for preliminary measurements of resistivity and helpful discussions. The work was supported by the Department of Atomic Energy (DAE), Government of India.

[1] A. E. Berkowitz, J. R. Mitchell, M. J. Carey, A. P. Young, S. Zhang, F. E. Spada, F. T. Parker, A. Hutten, and G. Thomas, Phys. Rev. Lett. **68**, 3745 (1992).
[2] J. Q. Xiao, J. S. Jiang, and C. L. Chien, Phys. Rev. Lett. **68**, 3749 (1992).
[3] J. Q. Xiao, J. S. Jiang, and C. L. Chien, Phys. Rev. B **46**, 9266 (1992).
[4] M. J. Carey, A. P. Young, A. Starr, D. Rao, and A. E. Berkowitz, Appl. Phys. Lett. **61**, 2935 (1992).
[5] C. L. Chien, J. Q. Xiao, and J. S. Jiang, J. Appl. Phys. **73**, 5309 (1993).
[6] S. Honda, M. Nawate, M. Tanaka, and T. Okada, J. Appl. Phys. **82**, 764 (1997).
[7] J. A. De Toro, J. P. Andrés, J. A. González, J. P. Goff, A. J. Barbero, and J. M. Riveiro, Phys. Rev. B **70**, 224412 (2004).
[8] K. Levin and D. Mills, Phys. Rev. B **9**, 2354 (1974).
[9] Y. Mei, E. H. Tyler, and H. L. Luo, Phys. Rev. B **26**, 4299 (1982).
[10] Y. Mei and H. L. Luo, Phys. Rev. B **34**, 509 (1986).
[11] J. Kondo, Prog. Theor. Phys. **32**, 37 (1964).
[12] J. R. Schrieffer and P. A. Wolff, Phys. Rev. **149**, 491 (1966).
[13] B. Coqblin and C. F. Ratto, Phys. Rev. Lett. **21**, 1065 (1968).
[14] B. Cornut and B. Coqblin, Phys. Rev. B **5**, 4541 (1972).
[15] C. Deenadas, A. W. Thompson, R. S. Craig, and W. E. Wallace, J. Phys. Chem. Solids **32**, 1853 (1971).
[16] C. D. Bredl, F. Steglich, and K. D. Schotte, J. Magn. Magn. Mater. **9**, 60 (1978).
[17] T. Komatsubara, T. Suzuki, M. Kawakami, S. Kunii, T. Fujita, Y. Isikawa, A. Takase, K. Kojima, M. Suzuki, Y. Aoki, K. Takegahara, and T. Kasuya, J. Magn. Magn. Mater. **15–18**, 963 (1980).
[18] S. Doniach, *Valence Instabilities and Related Narrow Band Phenomena*, edited by R. D. Parks (Plenum, New York, 1977), p. 169.
[19] L. M. Fabietti, J. Ferreyra, M. Villafuerte, S. E. Urreta, and S. P. Heluani, Phys. Rev. B **82**, 172410 (2010).
[20] A. Barman, M. Ghosh, S. Biswas, S. K. De, and S. Chatterjee, Solid State Commun. **106**, 691 (1998).
[21] A. Tiwari and K. P. Rajeev, Solid State Commun. **111**, 33 (1999).
[22] E. Rozenberg, M. Auslender, I. Felner, and G. Gorodetsky, J. Appl. Phys. **88**, 2578 (2000).
[23] D. Kumar, J. Sankar, J. Narayan, R. K. Singh, and A. K. Majumdar, Phys. Rev. B **65**, 094407 (2002).
[24] Y. Xu, J. Zhang, G. Cao, C. Jing, and S. Cao, Phys. Rev. B **73**, 224410 (2006).
[25] L. Maritato, C. Adamo, C. Barone, G. M. De Luca, A. Galdi, P. Orgiani, and A. Y. Petrov, Phys. Rev. B **73**, 094456 (2006).
[26] S. Mukhopadhyay and I. Das, Europhys. Lett. **79**, 67002 (2007).
[27] R. R. Jia, J. C. Zhang, R. K. Zheng, D. M. Deng, H.-U. Habermeier, H. L. W. Chan, H. S. Luo, and S. X. Cao, Phys. Rev. B **82**, 104418 (2010).
[28] S. Dhara, R. R. Chowdhury, S. Lahiri, P. Ray, and B. Bandyopadhyay, J. Magn. Magn. Mater. **374**, 647 (2015).
[29] J. M. D. Coey, A. E. Berkowitz, L. Balcells, F. F. Putris, and A. Barry, Phys. Rev. Lett. **80**, 3815 (1998).
[30] L. Balcells, J. Fontcuberta, B. Martinez, and X. Obradors, Phys. Rev. B **58**, R14697 (1998).
[31] P. Sheng, B. Abeles, and Y. Arie, Phys. Rev. Lett. **31**, 44 (1973).
[32] J. S. Helman and B. Abeles, Phys. Rev. Lett. **37**, 1429 (1976).
[33] O. Rapp, S. M. Bhagat, and H. Gudmundsson, Solid State Commun. **42**, 741 (1982).
[34] R. W. Cochrane and J. O. Strom-Olsen, Phys. Rev. B **29**, 1088 (1984).
[35] B. Sas, T. Kemeny, J. Toth, and F. I. B. Williams, Mater. Sci. Eng. **99**, 223 (1988).
[36] P. A. Lee and T. V. Ramakrishnan, Rev. Mod. Phys. **57**, 287 (1985).
[37] O. Ciftja, M. Luban, M. Auslender, and J. H. Luscombe, Phys. Rev. B **60**, 10122 (1999).
[38] M. I. Auslender, E. Rozenberg, A. E. Karlin, B. K. Chaudhuri, and G. Gorodetsky, J. Alloys Compd. **326**, 81 (2001).
[39] H. Sato, K. Honda, Y. Aoki, N. Kataoka, I. J. Kim, and K. Fukamichi, J. Magn. Magn. Mater. **152**, 109 (1996).
[40] S. B. Arnason, S. P. Herschfield, and A. F. Hebard, Phys. Rev. Lett. **81**, 3936 (1998).
[41] S. Dhara, R. R. Chowdhury, and B. Bandyopadhyay, RSC Adv. **5**, 95695 (2015).
[42] S. Legvold, D. T. Peterson, P. Burgardt, R. J. Hofer, B. Lundell, T. A. Vyrostek, and H. Girtner, Phys. Rev. B **9**, 2386 (1974).